Templating effect of Carbon Nanoforms on Highly Cross-Linked Imidazolium Network. Catalytic Activity of the Resulting Hybrids with Pd Nanoparticles

Vincenzo Campisciano,*[a] Carla Calabrese,[a,b] Leonarda Francesca Liotta,[c] Valeria La Parola,[c] Alberto Spinella,[d] Carmela Aprile,[b] Michelangelo Gruttadauria,*[a] and Francesco Giacalone*[a]

[a] *Dr. V. Campisciano, C. Calabrese, Prof. M. Gruttadauria, Prof. F. Giacalone*
Department of Biological, Chemical and Pharmaceutical Sciences and Technologies (STEBICEF), Università degli Studi di Palermo, V.le delle Scienze Ed. 17, 90128, Palermo, Italy.
E-mail: vincenzo.campisciano@unipa.it; michelangelo.gruttadauria@unipa.it; francesco.giacalone@unipa.it

[b] *C. Calabrese, Prof. C. Aprile*
Laboratory of Applied Material Chemistry (CMA), University of Namur, 61 rue de Bruxelles, 5000 Namur, Belgium.

[c] *Dr. L. F. Liotta, Dr. V. La Parola*

Istituto per lo Studio dei Materiali Nanostrutturati ISMN-CNR, Via Ugo La Malfa 153, 90146, Palermo, Italy.

[d] *Dr. A. Spinella*

Centro Grandi Apparecchiature-ATeN Center, Università degli Studi di Palermo, Via F. Marini 14, 90128, Palermo, Italy.

Abstract: Two different carbon nanoforms (CNFs), namely multi-walled carbon nanotubes (MWCNTs) and carbon nanohorns (CNHs), have been chosen as support for the direct polymerization of a bis-vinylimidazolium salt. TEM analyses revealed a templating effect of the CNFs on the growth of the polymeric network, which perfectly covers their whole surfaces creating a cylindrical or a spherical coating for MWCNTs and CNHs, respectively. Subsequently, the CNFs-polyimidazolium have been used as stabilizers for Pd nanoparticles (Pd NPs) and the obtained materials have been characterized by means of analytical and spectroscopic techniques, and then employed as easily recoverable and recyclable catalysts for Suzuki and Heck reactions. Quantitative conversions have been obtained in almost all the explored reactions, even employing low loading of catalyst (down to 0.007 mol%). Suzuki reactions were carried in pure water under aerobic conditions. Both materials showed excellent activity and recyclability for the investigated C-C coupling reactions with the CNHs-based material resulting slightly more active than the MWCNTs-based one due to a higher superficial exposure of Pd NPs.

Keywords: C-C coupling; Heck reaction; Heterogeneous catalysis; Nanotubes; Suzuki-Miyaura reaction

Introduction

Among the large number of supports employed in the field of heterogeneous catalysis, carbon nanoforms have played a key role due to their peculiar and advantageous features such as high surface area and thermal stability, exceptional mechanical resistance and unique electronic properties. Within CNFs family, fullerenes, carbon nanotubes (CNTs) and graphene are surely the most popular and studied members. They have been exploited in a plethora of applications such as energy conversion and storage,[1] electronics and optoelectronics,[1e, 2] sensing,[3] biomedicine,[4] and also the production of high performances materials such as films and fibers.[5] Conversely to the case of the above mentioned CNFs, the applications of another class of carbon allotropes, namely carbon nanohorns (CNHs), were less explored. CNHs are constituted by graphene tubes closed with a horn-shaped tip. By virtue of their structure, CNHs are very intriguing materials that share some features and chemistry resembling both that of fullerenes, due to the presence of the closed tips, and that of single-walled CNTs, thanks to their elongated shape. Among the possible applications of CNFs, catalysis is one of the most interesting emerging field.[6] In this context, transition metals catalyzed C-C coupling reactions play a central role both in academia and for synthesis of fine chemicals and pharmaceuticals. Palladium is probably the most versatile and used transition metal for catalyzed C-C couplings such as Suzuki, Heck and Sonogashira reactions.[7] The use of Pd nanoparticles (NPs) as heterogeneous catalysts of C-C coupling reactions have attracted increasing attention due to their intrinsically advantageous nature that combines high reactivity with very large surface area thanks to the high surface to volume ratio. Since the catalytic activity strongly depends on particles size and their distribution on support material,[8] an optimal interaction of Pd NPs with the support is a key priority. In the light of the weak interaction of metal NPs with pristine CNFs,

big efforts in functionalizing them have been made with the aim to obtain a better dispersion of catalytically active species on support surface and simultaneously promote the debundling of aggregates typical of CNTs and CNHs in their pristine form. Therefore, chemical modification of CNFs is an essential requirement to obtain catalytic materials with high activity and tailored for reducing the possible leaching of metal. Focusing attention on the covalent functionalization of CNTs and CNHs, the oxidative pre-treatment and the subsequent post-modification of such materials is surely the most employed method that provides access to a wide range of functionalities covalently grafted onto their surface. However, oxidative pre-treatment is not the only way to modify CNFs and other techniques to functionalize covalently pristine CNTs and CNHs were developed, which can involve addition of aryl diazonium salts, microwave-assisted functionalization, coating with polymers, among others.[9] In order to obtain highly active heterogeneous catalysts in which CNTs and CNHs can act as support materials of Pd NPs, the choice of a suitable stabilizer of metal NPs to avoid their aggregation during the preparation, deposition onto support or catalytic cycle is fundamental.[10]

Furthermore, the robustness of both CNTs and CNHs could ensure the recoverability and reusability of the catalyst. The interest in obtaining highly performing heterogeneous catalysts is witnessed by the many examples concerning the use of CNFs-Pd hybrid systems used for C–C coupling reactions. However, if on one hand it is possible to find a good number of examples about the use of CNTs-Pd hybrid systems in which CNTs were opportunely modified with different stabilizers of metal nanoparticles (MNPs) such as biguanide or imino-pyridine derivatives,[11] dendrimers,[12] Pd(II) complexes,[13] and many others,[14] on the other hand, CNHs were less used in this context.[15]

In continuation of our ongoing research on the use of imidazolium based catalysts and on the functionalization of different CNFs for catalytic purposes,[16] multi-walled carbon nanotubes (MWCNTs) and CNHs were chosen as support materials for Pd NPs. Among MNPs stabilizers, ionic liquids (ILs) play a central role. In particular imidazolium based ILs constitute an excellent medium in which MNPs are stabilized by means of both electrostatic and steric effects.[17] The

union of CNFs and ILs constitutes a successful marriage that results in a synergistic combination of the properties of both members to give hybrid systems with huge potential and applications.[14c, 16a, 16d, 18]

Herein, the radical polymerization of a bis-vinylimidazolium salt in presence of pristine MWCNTs and CNHs is reported.

The carbon nanoform structures acted as templates for the growth of the highly cross-linked imidazolium network polymer despite the random nature of the polymerization process. The obtained materials, which displayed a good dispersibility in water, were used as supports for the immobilization of Pd NPs and were tested as heterogeneous and recyclable catalysts for Suzuki reaction in aqueous medium and Heck coupling. The prepared hybrid materials were characterized by means of different techniques including thermogravimetric analysis (TGA), solid-state NMR spectroscopy, transmission electron microscopy (TEM), X-ray photoelectron spectroscopy (XPS) and microwave plasma – atomic emission spectrometry (MP-AES).

Experimental

Chemicals and solvents were purchased from commercial suppliers and used without further purification. For thin-layer chromatography (TLC), silica gel plates (Merck 60 F254) were used and compounds were visualized by irradiation with UV light and/or by treatment with a $KMnO_4$ solution. ^{1}H spectra were recorded with a Bruker 300 MHz spectrometer. The ^{13}C CPMAS NMR spectra were acquired by means of a spectrometer Bruker Avance II 400 operating at 400.15 and 100.63 MHz for ^{1}H and ^{13}C nuclides respectively and equipped with a 4 mm (H-X) double channel CPMAS probe. All spectra were acquired with a MAS speed of 8kHz, 1024 scans, a contact time of 2 ms, a delay time of 3 sec and an excitation pulse of 4.7 microseconds on the ^{1}H nucleus. The optimization of the Hartmann-Hahn condition has been obtained using an adamantane standard sample. This compound was also used as the external chemical shift reference. All samples were

placed in 4 mm zirconia rotors filled with Kel-F caps. Thermogravimetric analysis (TGA) was performed under nitrogen flow from 100 to 1000 °C with a heating rate of 10 °C min^{-1} in a Mettler Toledo TGA/DSC STAR System. TEM micrographs were recorded on a high-resolution transmission electron microscope (HRTEM) JEOL JEM-2100 operating at 200 kV accelerating voltage. Samples were dispersed in water and drop cast onto carbon coated copper TEM grids for HR-TEM analysis. The imaging conditions were carefully tuned by lowering the accelerating voltage of the microscope and reducing the beam current density to a minimum in order to minimize the electron beam induced damage of the sample. Microwave Plasma-Atomic Emission Spectroscopy (MP-AES) analyses were carried out with a 4200 MP-AES, Agilent. Analyses were conducted using a calibration curve, obtained by dilution. X-ray photoelectron spectroscopy (XPS) analyses were performed with a VGMicrotech ESCA 3000Multilab, equipped with a dual Mg/Al anode. The spectra were excited with the unmonochromatized Al Ka source (1486.6 eV) run at 14 kV and 15 mA. The analyzer was operated in the constant analyser energy (CAE) mode. For the individual peak energy regions, a pass energy of 20 eV set across the hemispheres was used. Survey spectra were measured at 50 eV pass energy. The sample powders were mounted on a double-sided adhesive tape. The pressure in the analysis chamber was in the range of 10^{-8} Torr during data collection. The constant charging of the samples was removed by referencing all the energies to the C1s set at 284.6 eV. The invariance of the peak shapes and widths at the beginning and at the end of the analyses ensured absence of differential charging. Analyses of the peaks were carried out with the software provided by VG, based on the non-linear least squares fitting program using a weighted sum of Lorentzian and Gaussian component curves after background subtraction according to Shirley and Sherwood.[19] Atomic concentrations were calculated from peak intensity using the sensitivity factors provided with the software. The binding energy values are quoted with a precision of ±0.15 eV and the atomic percentage with a precision of ±10%.

Synthesis of bis-vinylimidazolium salt 1: bis-vinylimidazolium salt **1** was prepared following a reported procedure with minor changes.[20] A solution of 1,4-dibromobutane (1.50 mL, 12.43 mmol)

and 1-vinylimidazole (2.45 mL, 26.53 mmol) in toluene (11 mL) was stirred at 90 °C. After 21 h a white precipitate was formed and toluene was removed by simple decantation. Afterwards, methanol was added and gently warmed to solubilize the solid. The volume was reduced by rotary evaporator obtaining a yellowish viscous oil that after addition of diethyl ether and sonication gave rise to a white precipitate. Diethyl ether was then removed and the white solid was further washed two times with diethyl ether and dried under vacuum at 40 °C. Bis-vinylimidazolium salt **1** was obtained as a white solid (4.516 g; 90%).

Synthesis of MWCNT-imi 2 and CNH-imi 4: In a two-neck round-bottom flask, a suspension of MWCNTs or CNHs (40 mg) and bis-vinylimidazolium salt **1** (674 mg, 1.67 mmol) in absolute ethanol (15 mL) was sonicated for 20 minutes. Afterwards, AIBN (28 mg, 0.17 mmol) was added and the mixture was degassed by bubbling argon for 20 minutes. The mixture was then heated at 78 °C while stirring under argon. After 20 h the mixture was filtered and the solid washed with methanol and diethyl ether. After drying under vacuum at 40 °C, MWCNT-imi **2** was obtained as a black/grey solid (617 mg) and CNH-imi **4** as a black solid (546 mg).

Synthesis of MWCNT-imi-Pd 3 and CNH-imi-Pd 5: $PdCl_2$ (37.57 mg, 0.21 mmol) and NaCl (246.68 mg, 4.20 mmol) were transferred in a round-bottom flask and water (15 mL) was added. The mixture was heated at 80 °C for 30 minutes until the formation of a brown solution. The obtained solution was allowed to reach the room temperature and was added dropwise to a stirring suspension of MWCNT-imi **2** or CNH-imi **4** (200 mg) in water (12.5 mL). The resulting mixture was stirred at room temperature for 22 h. The suspension was then filtered and the solid was washed with water, methanol and diethyl ether. Once dried, the resulting solid was suspended in absolute ethanol (15 mL) and sonicated for 15 minutes. After the sonication, the suspension was stirred and a freshly prepared suspension of $NaBH_4$ (56.74 mg, 1.47 mmol) in absolute ethanol (10 mL) was added dropwise under stirring to previous suspension. The resulting mixture was stirred at room temperature for 6 h. The suspension was then filtered and the resulting solid was washed with

water, methanol and acetone. After drying under vacuum at 40 °C, MWCNT-imi-Pd **3** and CNH-imi-Pd **5** were obtained as black solids (183 and 184 mg, respectively).

General procedure for the Suzuki reaction: Aryl bromide (0.5 mmol), boronic acid or phenylboronic acid pinacol ester (0.55 mmol), diisopropylamine (1 mmol), catalyst **3** (0.70 mg – 0.1 mol%) or **5** (0.52 mg – 0.07 mol%) and water (1.2 mL) were transferred in a glass vial with a screw cap and heated at 100 °C under stirring for the required time. Then, the reaction mixture was allowed to cool down to room temperature, diluted with water and extracted three times with dichloromethane. The combined organic layers were dried with anhydrous Na_2SO_4 and the solvent was evaporated under vacuum. The residue was filtered by a short pad of silica using a mixture of hexane and ethyl acetate as eluent. The conversions were estimated by ^{1}H NMR spectroscopy.

General recycling procedure in the Suzuki reaction: 4-bromoacetophenone (1 mmol), phenylboronic acid (1.1 mmol), diisopropylamine (2 mmol), catalyst **3** (1.40 mg – 0.1 mol%) or **5** (1.05 mg – 0.07 mol%) and water (2.4 mL) were transferred in a glass vial with a screw cap and heated at 100 °C under stirring. After 3h the reaction mixture was allowed to cool down to room temperature, diluted with ethyl acetate and centrifuged. Organic layer was recovered and catalyst was further washed two times with ethyl acetate, then with a mixture of methanol/ethyl acetate 2:1 and finally with diethyl ether. Once dry, the catalyst was used in the next cycle. The recovered organic layers were combined and evaporated under reduced pressure, diluted with water and extracted three times with dichloromethane. The combined organic layers were then dried with anhydrous Na_2SO_4 and the solvent was evaporated under vacuum. The residue was purified by column chromatography using a mixture of hexane and ethyl acetate as eluent.

General procedure for the Heck reaction: Aryl iodide (0.5 mmol), alkene (0.75 mmol), triethylamine (1 mmol), catalyst **3** (0.70 mg – 0.1 mol%) or **5** (0.52 mg – 0.07 mol%) and DMF (1 mL) were transferred in a glass vial with a screw cap and heated at 120 °C under stirring for the required time. Then, the reaction mixture was allowed to cool down to room temperature, diluted

with water and extracted three times with diethyl ether. The combined organic layers were dried with anhydrous Na_2SO_4 and the solvent was evaporated under vacuum. The residue was filtered by a short pad of silica using a mixture of hexane and ethyl acetate as eluent. The conversions were estimated by ^1H NMR spectroscopy.

General recycling procedure in the Heck reaction: 4-iodoanisole (1 mmol), methyl acrylate (1.5 mmol), triethylamine (2 mmol), catalyst **3** (1.40 mg – 0.1 mol%) or **5** (1.05 mg – 0.07 mol%) and DMF (2 mL) were transferred in a glass vial with a screw cap and heated at 120 °C under stirring. After 3h the reaction mixture was allowed to cool down to room temperature, diluted with diethyl ether and centrifuged. Organic layer was recovered and catalyst was further washed with diethyl ether, and then four times with methanol, water, methanol again and finally with diethyl ether. Once dry, the catalyst was used in the next cycle. The recovered organic layers were combined and evaporated under reduced pressure, diluted with water and extracted three times with diethyl ether. The combined organic layers were then dried with anhydrous Na_2SO_4 and the solvent was evaporated under vacuum. The residue was purified by column chromatography using a mixture of hexane and ethyl acetate as eluent.

Results and Discussion

Hybrid materials **3** and **5** were easily prepared through the straightforward synthetic strategy depicted in **Scheme 1**. Radical polymerization of bis-vinylimidazolium salt **1**[20] onto the MWCNTs and CNHs surface was started by thermal decomposition of radical initiator 2,2'-azobis(2-methylpropionitrile) (AIBN) in ethanol, at reflux. The obtained poly-imidazolium salt coated materials, namely MWCNT-imi **2** and CNH-imi **4**, were dispersed in water in the presence of Na_2PdCl_4 to proceed with ion-exchange of bromides with tetrachloropalladate ions, followed by reduction with $NaBH_4$ in ethanol leading to the final materials MWCNT-imi-Pd **3** and CNH-imi-Pd **5**, respectively (**Scheme 1**).

Scheme 1. Synthetic procedure for the preparation of materials MWCNT-imi-Pd **3** an d CNH-imi-Pd **5**.

It is worth noting that the above approach represents a versatile strategy to accede to a number of heterogeneous catalysts, given that different metal nanoparticle precursors can be adopted and stabilized or even polyoxometalate species can be immobilized through ionic-exchange. The poly-imidazolium salt loadings of materials MWCNT-imi **2** and CNH-imi **4** were estimated by means of TGA under N_2 by considering the weight losses at 700 °C corresponding to 92.5 and 88.6 wt%, respectively (**Figure 1**).

Figure 1. TGA profiles under N_2 of pristine (dashed lines) and functionalized (solid lines) MWCNTs and CNHs.

TGA profiles of pristine MWCNTs and CNHs showed very low weight losses at the same temperature corresponding to 2.8 and 3.3 wt%, respectively. Therefore, the calculated poly-imidazolium salt loading of materials MWCNTs-imi **2** and CNH-imi **4** correspond to 2.28 and 2.13 mmol/g, respectively.

^{13}C Cross-polarization magic angle spinning NMR (^{13}C CPMAS NMR) spectra of all materials MWCNT-imi **2**, MWCNT-imi-Pd **3**, CNH-imi **4** and CNH-imi-Pd **5** were recorded (**Figure 2**).

Figure 2. ^{13}C CPMAS NMR spectra of materials MWCNT-imi **2**, MWCNT-imi-Pd **3**, CNH-imi **4** and CNH-imi-Pd **5**.

^{13}C CPMAS NMR spectra of materials **2** and **4** confirmed the good outcoming of the polymerization step as evidenced by the absence of signals which can be ascribed to residual vinyl groups at around 110 ppm (**Figure 2** – red lines). On the other hand, the signals at low fields (120-140 ppm) attributed to the carbon atoms of the imidazolium rings and those of aliphatic carbon

atoms resonating in the 20-60 ppm region are clearly visible. NMR spectra of the final hybrids decorated with Pd NPs, namely MWCNT-imi-Pd **3** and CNH-imi-Pd **5**, showed no relevant difference with the spectra of their precursors (compare red lines with black lines in **Figure 2**).

In **Figure 3** high-resolution transmission electron microscopy (HRTEM) micrographs of pristine MWCNTs, MWCNT-imi **2** and MWCNT-imi-Pd **3** and CNHs, CNH-imi **4** and CNH-imi-Pd **5** are displayed. Pristine MWCNTs are aggregated forming ropes and bundles (**Figure 3a**). However, polymerization of bis-vinylimidazolium salt leads to a better dispersion of the CNTs, which are almost all uniformly wrapped by poly-imidazolium salt network (Poly-imi) that creates a perfect cylindrical coating with a mean outer diameter of ~100 nm (**Figure 3b** and **S1a-b**). Similar results were obtained by Li, Chen *et al.* that functionalized MWCNTs with a methylimidazolium salt derivative by free-radical polymerization.[18l] It is noteworthy to point out that polymerization of bis-vinylmidazolium salts onto different supports, such as silica, could result in a physical mixture composed of supported Poly-imi and homopolymerized imidazolium salt, as previously reported.[21] Herein, no traces of isolated domains of homopolymer were found. This finding could be explained considering that CNTs can act as a sort of templating agent that leads the polymerization of the bis-vinylmidazolium salt monomer to take place around the nanotubes skeleton. TEM images of CNH-imi **4** (**Figure 3f**, and **S2a-b**) showed also that functionalization of CNHs with bis-vinylmidazolium salt **1** led to the formation of a homogeneous spherical-like coating of Poly-imi uniformly distributed onto the surface of CNHs. On the other hand, only at high magnifications it was possible to observe the presence of very small Pd NPs uniformly distributed onto the 3D Poly-imi network of MWCNT-imi-Pd **3**, whose dimensions could not be determined (**Figure 3d** and **S1d**). Conversely, on CNH-imi-Pd **5** Pd NP are clearly visible (**Figure 3g-h** and **S2c-e**), showing a bimodal distribution with a mean particle size of 28.8 ± 12.0 nm (n = 66) and 2.6 ± 0.6 nm (n = 282) (**Figure S2f**), for the big and the small NPs, respectively. It is interesting to note that in this case the NPs are mainly located on the outer part of the hybrid material being thus more available for the catalysis.

Figure 3. Representative HRTEM images of a) pristine MWCNT, b) MWCNT-imi **2**, c-d) MWCNT-imi-Pd **3**, e) pristine CNHs, f) CNH-imi **4**, g-h) CNH-imi-Pd **5**.

Palladium loading of materials MWCNT-imi-Pd **3** and CNH-imi-Pd **5** was determined by means of microwave plasma – atomic emission spectrometry (MP-AES) and was found to be 7.6 and 7.1 wt%, respectively.

Furthermore, materials MWCNT-imi-Pd **3** and CNH-imi-Pd **5** were subjected to X-ray photoelectron spectroscopy (XPS) analysis (**Figure 4**) to estimate the degree of reduction of palladium after the treatment with $NaBH_4$. The results, summarized in **Table 1**, showed how the degree of reduction was quite similar for both materials being the content of Pd(0) equal to 61 and 63% for MWCNT-imi-Pd **3** and CNH-imi-Pd **5**, respectively.[22] Moreover, it is worth to note that although the palladium loading of material **3** is slightly higher than that of **5** (7.6 *vs* 7.1 wt%), the Pd/C atomic ratio determined by XPS is the same revealing a higher surface exposure of Pd NPs in the latter hybrid (**Table 1**). This finding is in agreement with HRTEM analysis.

Figure 4. High-resolution XPS of the Pd3d region of materials MWCNT-imi-Pd **3** and CNH-imi-Pd **5**.

Table 1. $Pd3d_{5/2}$ binding energies (eV), relative percentages (%) and Pd/C atomic ratios of MWCNT-imi-Pd **3** and CNH-imi-Pd **5**.

Once the materials were fully characterized, MWCNT-imi-Pd **3**, and CNH-imi-Pd **5** were initially tested in the catalysis of the Suzuki reaction. Firstly, MWCNT-imi-Pd **3** was tested in water, at 100 °C, in the presence of K_2CO_3 as base, affording 70% of conversion into the biphenyl-4-carboxaldehyde in 6 h (**Table 2**, **Entry 1**). After the same reaction time, a lower conversion (42%) was recorded by using ethanol as solvent, at 50 °C (**Entry 2**). On the other hand, when the reaction was run in 3 h in a mixture of H_2O/EtOH (1:1 v/v) at 50 °C, the conversion into the desired product

was complete (**Entry 3**). No relevant improvements were observed when K_3PO_4 was used as base in water at 100 °C. The obtained results were quite similar to those collected with K_2CO_3 (compare **entries 1** and **4**). However, the use of diisopropylamine (DIPA) in water at 100 °C gave rise to full conversion in only 2 h (**Entry 5**). Then, the optimized reaction conditions were employed in the Suzuki reaction using the less reactive 4-bromoanisole. Data reported in Table 2 prove that the best conditions arise from the combination of DIPA as base and water as solvent. (compare **entries 6** and **7**). On the grounds of this finding, CNH-Imi-Pd **5** was tested at 0.1 mol%, using DIPA as base and water as solvent showing a higher catalytic activity than MWCNT-imi-Pd **3** (**Entries 7-8**). Therefore, in the light of the obtained results, the catalytic loading of CNH-imi-Pd **5** was further decreased to 0.07 mol%. Despite the lower catalytic loading, catalyst **5** allowed to obtain high conversions into the corresponding biphenyls when both 4-bromoanisole and 4-bromobenzaldehyde were used (**Entries 9-10**).

Table 2. Screening of reaction conditions for the Suzuki–Miyaura reaction.

The previously optimized reaction conditions were selected to check the catalytic versatility of the solids **3** and **5** in the Suzuki couplings between a broad spectrum of substrates including several aryl bromides, one aryl chloride, boronic acids and one pinacol ester (Table 3). In this context, MWCNT-Imi-Pd **3** and CNH-Imi-Pd **5** were tested using a Pd loading of 0.1 and 0.07 mol%, respectively. (**Table 3**).

Table 3. Suzuki–Miyaura reactions catalyzed by materials MWCNT-imi-Pd **3** and CNH-imi-Pd **5**.

Conversions in the corresponding biphenyls were from good to excellent in almost all the cases with both catalysts being CNH-imi-Pd **5** slightly more active than MWCNT-imi-Pd **3**. This difference in activity is more pronounced when 3-bromotoluene was reacted with phenylboronic

acid or the electron rich 4-bromoanisole was coupled with 2-tolylboronic acid (**Table 3**, **Entries 5** and **6**).

Conversely, it is noteworthy to note that using phenylboronic acid pinacol ester or 4-formylphenylboronic acid in combination with 4-bromoacetophenone and 4-bromoanisole, respectively (**Entries 8** and **9**), the catalytic performances of both materials resulted to be quite similar. However, CNH-imi-Pd **5** still showed a slightly higher activity than MWCNT-imi-Pd **3** because of the lower catalytic loading employed that allows it to reach a higher turnover number (TON, defined as moles of aryl halide converted/moles of palladium) value even when conversion into the desired product was lower than the MWCNTs based catalyst was used (**Entry 9**; TONs values: 470 and 514). The somewhat different catalytic activity may be rationalized as a result of different contributions: although MWCNT-imi-Pd **3** has both a higher Pd content and lower Pd NPs dimensions, the palladium seems to be uniformly distributed in the 3D polymeric network, being the inner layers less available to the catalysis. On the contrary, CNH-imi-Pd **5** has lower Pd content and higher NPs size but the Pd NPs are mainly exposed on the surface and easily accessible to the reactants during the catalysis.

A further experiment was performed by using a reduced catalytic loading. The reaction between 4-bromoacetophenone and phenylboronic acid was chosen for this purpose. In particular, catalyst MWCNT-imi-Pd **3** was tested at 0.01 mol%, whereas CNH-Imi-Pd **5** was employed with a palladium loading of 0.007 mol% (**Table 3**, **Entry 11**). This reaction confirmed the different activity of the two catalysts. After 16 h MWCNT-imi-Pd **3** gave 95% of conversion, whereas, in the same time, CNH-imi-Pd **5** allowed to a full conversion into the corresponding product. Taking into account the different catalytic loading, it is noteworthy to mention the reached TONs values, namely 9500 and 14286 for catalyst **3** and **5**, respectively, which highlight the different catalytic activity of the two catalysts. Furthermore, an aryl chloride, 1-choro-4-nitrobenzene was tested in the Suzuki reaction in the presence of catalyst **5** (Table 3, entry 12). It worked with a conversion of 39%, which is remarkable as 1-chloro-4-nitrobenzene has a significantly lower reactivity than the

aryl bromides. Still the result is not optimized yet. To obtain higher conversion, the amount of the catalyst could be increased or harsher reaction conditions could be applied.

In **Table 4** a comparison between the more active CNH-imi-Pd **5** and other catalytic systems reported elsewhere in the Suzuki reaction between 4-bromoanisole and phenylboronic acid is shown, although a strictly direct comparison is not possible since the majority of the reactions were not carried out in pure water as in our case. Examples concerning both Pd(II) complexes and Pd NPs supported onto SWCNTs, MWCNTs, and oxidized CNHs were taken into account. **Table 4** shows that CNH-imi-Pd **5** exhibits higher or comparable activity with the other examined examples. Furthermore, it was possible to compare the catalytic activity of the herein presented system CNH-imi-Pd **5** with commercial Pd/C catalyst used in the same reaction conditions (water, DIPA, 100 °C). In the case of Pd/C, a 93% of yield into the corresponding biphenyl derivative was obtained in just twenty minutes, but an over twenty-fold higher Pd loading than that used in the case of CNH-imi-Pd **5** was employed (compare **entries 12** and **13**).

Table 4. Comparison between CNH-imi-Pd **5** and other reported catalytic systems in the Suzuki–Miyaura coupling of 4-bromoanisole with phenylboronic acid.

The recyclability of MWCNT-imi-Pd **3** and CNH-imi-Pd **5**, at 0.1 and 0.07 mol% respectively, was investigated in the Suzuki reaction between 4-bromoacetophenone and phenylboronic acid. Both catalysts retained their activity over five cycles affording the desired product in quantitative yield.

Furthermore, MWCNT-imi-Pd **3** and CNH-imi-Pd **5** were tested in the catalysis of the Heck reaction with the same loading used for the Suzuki reaction (0.1 and 0.07 mol%, respectively). Both electron rich and electron poor aryl iodides were reacted with different alkenes, such as styrene, 4-chlorostyrene and methyl acrylate using dimethylformamide as solvent and triethylamine (TEA) as base at 120 °C. The conversions into the corresponding products were from good to excellent (**Table 5**). Once again, taking into account its lower catalytic loading, CNH-imi-Pd **5** showed a higher activity than MWCNT-imi-Pd **3**, especially when styrene and 4-chlorostyrene were used

(**Entries 1-10**). Moreover, 4-bromobenzaldehyde was coupled with styrene affording good results (**Entry 10**) and with methyl acrylate affording excellent results (**Entry 19**).

Table 5. Mizoroki–Heck reactions catalyzed by materials MWCNT-imi-Pd **3** and CNH-imi-Pd **5**.

Regioselectivity towards *trans* alkene isomer in the Heck reaction between methyl acrylate and several aryl iodides was excellent and no traces of by-products were detected (**Entries 11-19**). However, when styrene and 4-chlorostyrene were employed, the regioselectivity was lower with the formation of the corresponding *gem*-alkenes in variable amounts between 2 and 15 mol% (**Entries 1-10**).

A further experiment with a tenfold lower catalytic loading was carried out using MWCNT-imi-Pd **3** and CNH-imi-Pd **5** (0.01 and 0.007 mol%, respectively) in the reaction between 4-iodoanisole and methyl acrylate (**Entry 20**). In the adopted conditions, these low loading allowed to a quantitative conversion into the desired product after 5 h.

Furthermore, the same reaction between 4-iodoanisole and methyl acrylate was chosen to assess the recyclability of MWCNT-imi-Pd **3** and CNH- imi-Pd **5** with a Pd loading of 0.1 and 0.07 mol%, respectively. Both catalysts gave rise to complete conversion into the corresponding product over the six cycles investigated. At the end of each catalytic run, the solids were simply recovered by centrifugation and successfully reused retaining their catalytic activity. No catalytic activity was observed in the recovered solution.

Conclusion

In conclusion, we have applied a straightforward approach based on the direct radical polymerization of a bis-vinylimidazolium dibromide salt in the presence of different pristine carbon nanoforms, namely multi-walled carbon nanotubes and carbon nanohorns, which allowed obtaining two CNFs-polyimidazolium hybrids. Interestingly, in both cases, the carbon nanoform structures acted as templates for the growth of the highly cross-linked imidazolium network polymer despite

the random nature of the polymerization process. The hybrids were hence employed as new supports and stabilizers for palladium-nanoparticles and the resulting materials were characterized by means of TGA, ^{13}C CPMAS NMR, MP-AES, XPS and HRTEM. This latter technique revealed two different situations regarding both the dimensions and the distribution of Pd NPs on the materials MWCNT-imi-Pd **3** and CNH-imi-Pd **5**. If on the one hand, only at high magnifications, it was possible to observe the presence of very small Pd NPs uniformly distributed onto material **3**, on the other hand, material **5** is characterized by the presence of bigger Pd NPs mainly allocated on the outer part of the hybrid material. Because of the small size of Pd Nps dispersed onto material **3**, it was not possible to estimate their mean dimensions. On the contrary, material **5** showed a bimodal distribution with a mean particle size of 28.8 ± 12.0 nm and 2.6 ± 0.6 nm. Considering the similar imidazolium loading on materials **3** and **5**, such difference could be ascribed to the different morphology and symmetry of the two carbon nanoforms. The two catalysts, MWCNT-imi-Pd **3** and CNH-imi-Pd **5**, were then extensively used with a large set of substrates in the Suzuki reactions in pure water under air atmosphere and in the Heck reactions in 0.1 and 0.07 mol% loading respectively, giving C-C coupled products in high conversions. In the case of Suzuki reactions in pure water, results were comparable or even better than those obtained with commercial Pd/C[31] or other supported Pd-based catalysts.[11a, 13a, 15a, 23-30, 32] Both catalysts were recovered after centrifugation and reused up to five cycles without loss in catalytic activity. Moreover, the catalytic loading was also scaled down to 0.01 and 0.007 mol% for MWCNT-imi-Pd **3** and CNH-imi-Pd **5** respectively, still giving high TON values. Carbon nanohorns-based material proved to be a slightly more active catalyst for the investigated C-C coupling reactions probably for a favourable balance between Pd nanoparticle size and their complete exposure to the reactants. The simple preparation, the high catalytic activity even in consecutive cycles make such catalysts interesting for application in large scale and for continuous flow conditions.

Acknowledgements

Financial support from the University of Palermo is gratefully acknowledged. The authors are also very grateful to Dr. Giorgio Nasillo for his valuable work with TEM measurements provided by ATeN Center - University of Palermo.

References

[1] a) L. Dai, D. W. Chang, J.-B. Baek, W. Lu, *Small* **2012**, *8*, 1130-1166; b) Z. Yang, J. Ren, Z. Zhang, X. Chen, G. Guan, L. Qiu, Y. Zhang, H. Peng, *Chem. Rev.* **2015**, *115*, 5159-5223; c) L. Liu, Z. Niu, J. Chen, *Chem. Soc. Rev.* **2016**, *45*, 4340-4363; d) Q. Wu, L. Yang, X. Wang, Z. Hu, *Acc. Chem. Res.* **2017**, *50*, 435-444; e) D. Jariwala, V. K. Sangwan, L. J. Lauhon, T. J. Marks, M. C. Hersam, *Chem. Soc. Rev.* **2013**, *42*, 2824-2860.

[2] a) A. Kamyshny, S. Magdassi, *Small* **2014**, *10*, 3515-3535; b) E. B. Secor, M. C. Hersam, *J. Phys. Chem. Lett.* **2015**, *6*, 620-626.

[3] a) S. N. Kim, J. F. Rusling, F. Papadimitrakopoulos, *Adv. Mater.* **2007**, *19*, 3214-3228; b) Y. Yang, X. Yang, Y. Yang, Q. Yuan, *Carbon* **2018**, *129*, 380-395.

[4] a) A. Chen, S. Chatterjee, *Chem. Soc. Rev.* **2013**, *42*, 5425-5438; b) C. Cha, S. R. Shin, N. Annabi, M. R. Dokmeci, A. Khademhosseini, *ACS Nano* **2013**, *7*, 2891-2897; c) N. L. Teradal, R. Jelinek, *Adv. Healthc. Mater.* **2017**, *6*, 1700574; d) H. Liu, L. Zhang, M. Yan, J. Yu, *J. Mater. Chem. B* **2017**, *5*, 6437-6450.

[5] D. Janas, K. K. Koziol, *Nanoscale* **2016**, *8*, 19475-19490.

[6] V. Campisciano, M. Gruttadauria, F. Giacalone, *ChemCatChem*, **2019**, *11*, 90-133.

[7] a) H.-U. Blaser, A. Indolese, A. Schnyder, H. Steiner, M. Studer, *J. Mol. Catal. A: Chem.* **2001**, *173*, 3-18; b) Yin, J. Liebscher, *Chem. Rev.* **2007**, *107*, 133-173; c) D. Astruc, *Inorg. Chem.* **2007**, *46*, 1884-1894; d) V. Polshettiwar, A. Decottignies, C. Len, A. Fihri, *ChemSusChem* **2010**, *3*, 502-522; e) Á. Molnár, *Chem. Rev.* **2011**, *111*, 2251-2320; f) A. Balanta, C. Godard, C. Claver, *Chem. Soc. Rev.* **2011**, *40*, 4973-4985; g) A. Suzuki, *Angew. Chem. Int. Ed.* **2011**, *50*, 6722-6737; h) E.-i. Negishi, *Angew. Chem. Int. Ed.* **2011**, *50*, 6738-6764; i) C. Deraedt, D. Astruc, *Acc. Chem. Res.* **2014**, *47*, 494-503.

[8] M. Pérez-Lorenzo, *J. Phys. Chem. Lett.* **2012**, *3*, 167-174.

[9] a) E. Vázquez, F. Giacalone, M. Prato, *Chem. Soc. Rev.* **2014**, *43*, 58-69; b) Y. Yan, J. Miao, Z. Yang, F.-X. Xiao, H. B. Yang, B. Liu, Y. Yang, *Chem. Soc. Rev.* **2015**, *44*, 3295-3346; c) N. Karousis, I. Suarez-Martinez, C. P. Ewels, N. Tagmatarchis, *Chem. Rev.* **2016**, *116*, 4850-4883.

[10] a) M. Moreno-Mañas, R. Pleixats, *Acc. Chem. Res.* **2003**, *36*, 638-643; b) D. Astruc, F. Lu, J. R. Aranzaes, *Angew. Chem. Int. Ed.* **2005**, *44*, 7852-7872.

[11] a) H. Veisi, A. Khazaei, M. Safaei, D. Kordestani, *J. Mol. Catal. A: Chem.* **2014**, *382*, 106-113; b) M. Adib, R. Karimi-Nami, H. Veisi, *New J. Chem.* **2016**, *40*, 4945-4951.

[12] a) M. R. Nabid, Y. Bide, S. J. Tabatabaei Rezaei, *Appl. Catal., A* **2011**, *406*, 124-132; b) F. Giacalone, V. Campisciano, C. Calabrese, V. La Parola, Z. Syrgiannis, M. Prato, M. Gruttadauria, *ACS Nano* **2016**, *10*, 4627-4636.

[13] a) M. Navidi, N. Rezaei, B. Movassagh, *J. Organomet. Chem.* **2013**, *743*, 63-69; b) B. Movassagh, F. S. Parvis, M. Navidi, *Appl. Organomet. Chem.* **2015**, *29*, 40-44.

[14] a) S. Mahouche Chergui, A. Ledebt, F. Mammeri, F. Herbst, B. Carbonnier, H. Ben Romdhane, M. Delamar, M. M. Chehimi, *Langmuir* **2010**, *26*, 16115-16121; b) J. Y. Kim, K. Park, S. Y. Bae, G. C. Kim, S. Lee, H. C. Choi, *J. Mater. Chem.* **2011**, *21*, 5999-6005; c) L. Rodríguez-Pérez, C. Pradel, P. Serp, M. Gómez, E. Teuma, *ChemCatChem* **2011**, *3*, 749-

754; d) E. Kim, H. S. Jeong, B. M. Kim, *Catal. Commun.* **2014**, *46*, 71-74; e) D. V. Jawale, E. Gravel, C. Boudet, N. Shah, V. Geertsen, H. Li, I. N. N. Namboothiri, E. Doris, *Catal. Sci. Technol.* **2015**, *5*, 2388-2392; f) A. H. Labulo, B. S. Martincigh, B. Omondi, V. O. Nyamori, *J. Mater. Sci.* **2017**, *52*, 9225-9248.

[15] a) T. Itoh, H. Danjo, W. Sasaki, K. Urita, E. Bekyarova, M. Arai, T. Imamoto, M. Yudasaka, S. Iijima, H. Kanoh, K. Kaneko, *Carbon* **2008**, *46*, 172-175; b) N. Karousis, T. Ichihashi, M. Yudasaka, S. Iijima, N. Tagmatarchis, *J. Nanosci. Nanotechnol.* **2009**, *9*, 6047-6054.

[16] a) M. Buaki-Sogo, A. Vivian, L. A. Bivona, H. Garcia, M. Gruttadauria, C. Aprile, *Catal. Sci. Technol.* **2016**, *6*, 8418-8427; b) F. Giacalone, M. Gruttadauria, *ChemCatChem* **2016**, *8*, 664-684; c) F. Giacalone, V. Campisciano, C. Calabrese, V. La Parola, L. F. Liotta, C. Aprile, M. Gruttadauria, *J. Mater. Chem. A* **2016**, *4*, 17193-17206; d) C. Calabrese, L. F. Liotta, E. Carbonell, F. Giacalone, M. Gruttadauria, C. Aprile, *ChemSusChem* **2017**, *10*, 1202-1209; e) V. Campisciano, F. Giacalone, M. Gruttadauria, *Chem. Rec.* **2017**, *17*, 918-938.

[17] a) M.-A. Neouze, *J. Mater. Chem.* **2010**, *20*, 9593-9607; b) C. J. Serpell, J. Cookson, A. L. Thompson, C. M. Brown, P. D. Beer, *Dalton Trans.* **2013**, *42*, 1385-1393.

[18] a) M. J. Park, J. K. Lee, B. S. Lee, Y. W. Lee, I. S. Choi, S. G. Lee, *Chem. Mater.* **2006**, *18*, 1546-1551; b) T. Fukushima, T. Aida, *Chem. Eur. J.* **2007**, *13*, 5048-5058; c) R. T. Kachoosangi, M. M. Musameh, I. Abu-Yousef, J. M. Yousef, S. M. Kanan, L. Xiao, S. G. Davies, A. Russell, R. G. Compton, *Anal. Chem.* **2009**, *81*, 435-442; d) S. Guo, S. Dong, E. Wang, *Adv. Mater.* **2010**, *22*, 1269-1272; e) J. Y. Shin, Y. S. Kim, Y. Lee, J. H. Shim, C. Lee, S. G. Lee, *Chem. Asian J.* **2011**, *6*, 2016-2021; f) Y. Kuang, B. Wu, D. Hu, X. Zhang, J. Chen, *J. Solid State Electrochem.* **2012**, *16*, 759-766; g) M. Tunckol, J. Durand, P. Serp, *Carbon* **2012**, *50*, 4303-4334; h) M. Tunckol, S. Fantini, F. Malbosc, J. Durand, P. Serp, *Carbon* **2013**, *57*, 209-216; i) S. Li, Z. Dong, H. Yang, S. Guo, G. Gou, R. Ren, Z. Zhu, J. Jin, J. Ma, *Chem. Eur. J.* **2013**, *19*, 2384-2391; j) S. Lee, J. Y. Shin, S. G. Lee, *Tetrahedron Lett.* **2013**, *54*, 684-687; k) A. R. Hajipour, Z. Khorsandi, H. Karimi, *Appl. Organomet. Chem.* **2015**, *29*, 805-808; l) Y. Ren, Z. Zhou, G. Yin, G. X. Chen, Q. Li, *Mater. Lett.* **2016**, *166*, 133-136.

[19] D. A. Shirley, *Phys. Rev. B* **1972**, *5*, 4709-4714.

[20] P. Agrigento, S. M. Al-Amsyar, B. Soree, M. Taherimehr, M. Gruttadauria, C. Aprile, P. P. Pescarmona, *Catal. Sci. Technol.* **2014**, *4*, 1598-1607.

[21] H. A. Beejapur, F. Giacalone, R. Noto, P. Franchi, M. Lucarini, M. Gruttadauria, *ChemCatChem* **2013**, *5*, 2991-2999.

[22] M. Gholinejad, M. Bahrami, C. Nájera, *Molecular Catalysis* **2017**, *433*, 12-19.

[23] R. Ghorbani-Vaghei, S. Hemmati, M. Hashemi, H. Veisi, *C. R. Chim.* **2015**, *18*, 636-643.

[24] A. R. Hajipour, Z. Khorsandi, *Appl. Organomet. Chem.* **2016**, *30*, 256-261. In this paper authors claim to use a catalytic loading of 0.0022 mol% of Pd, which is, actually, incorrect since the Pd loading is 0.3 mmol/g.

[25] D. Khalili, A. R. Banazadeh, E. Etemadi-Davan, *Catal. Lett.* **2017**, *147*, 2674-2687.

[26] A. Ohtaka, J. M. Sansano, C. Nájera, I. Miguel-García, Á. Berenguer-Murcia, D. Cazorla-Amorós, *ChemCatChem* **2015**, *7*, 1841-1847.

[27] P.-P. Zhang, X.-X. Zhang, H.-X. Sun, R.-H. Liu, B. Wang, Y.-H. Lin, *Tetrahedron Lett.* **2009**, *50*, 4455-4458.

[28] F. Yang, C. Chi, S. Dong, C. Wang, X. Jia, L. Ren, Y. Zhang, L. Zhang, Y. Li, *Catal. Today* **2015**, *256*, 186-192.

[29] H.-q. Song, Q. Zhu, X.-j. Zheng, X.-g. Chen, *J. Mater. Chem. A* **2015**, *3*, 10368-10377.

[30] H. Veisi, R. Azadbakht, F. Saeidifar, M. R. Abdi, *Catal. Lett.* **2017**, *147*, 976-986.

[31] X. Rao, C. Liu, Y. Zhang, Z. Gao, Z. Jin, *Chin. J. Catal.* **2014**, *35*, 357-361.

[32] a) G. Park, S. Lee, S. J. Son, S. Shin, *Green Chem.* **2013**, *15*, 3468-3473; b) A. Chatterjee, T. R. Ward, *Catal. Lett.* **2016**, *146*, 820-840; c) D. Zhang, C. Zhou, R. Wang, *Catal.*

Commun. **2012**, *22*, 83-88; d) M. Lamblin, L. Nassar-Hardy, J.-C. Hierso, E. Fouquet, F.-X. Felpin, *Adv. Synth. Catal.* **2010**, *352*, 33-79.

Table 1. $Pd3d_{5/2}$ binding energies (eV), relative percentages (%) and Pd/C atomic ratios of MWCNT-imi-Pd **3** and CNH-imi-Pd **5**.

	MWCNT-imi-Pd **3**	CNH-imi-Pd **5**
Pd(0)	335.3 (61)	334.7 (63)
Pd(II)	337.6 (39)	337.3 (37)
Pd/C	0.016	0.016

Table 2. Screening of reaction conditions for the Suzuki–Miyaura reaction.[a]

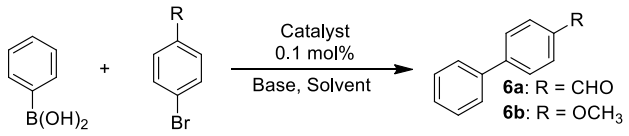

Entry	Catalyst	R	Base	T (°C)	t (h)	Conv. (%)[b]	Solvent
1	**3**	CHO	K_2CO_3	100	6	70	H_2O
2	**3**	CHO	K_2CO_3	50	6	42	EtOH
3	**3**	CHO	K_2CO_3	50	3	99	H_2O/EtOH (1:1)
4	**3**	CHO	K_3PO_4	100	6	75	H_2O
5	**3**	CHO	DIPA	100	2	99	H_2O
6	**3**	OCH_3	K_2CO_3	50	5	36	H_2O/EtOH (1:1)
7	**3**	OCH_3	DIPA	100	1	87	H_2O
8	**5**	OCH_3	DIPA	100	1	99	H_2O
9[c]	**5**	OCH_3	DIPA	100	1	93	H_2O
10[c]	**5**	CHO	DIPA	100	2	99	H_2O

[a] Reaction conditions: aryl bromide (0.5 mmol), phenylboronic acid (0.55 mmol), base (2 equiv.), catalyst (0.1 mol%), solvent (1.2 mL). [b] Conversion determined by ^1H NMR. [c] CNH-imi-Pd **5**

used at 0.07 mol%.

Table 3. Suzuki–Miyaura reactions catalyzed by materials MWCNT-imi-Pd **3** and CNH-imi-Pd **5**.[a]

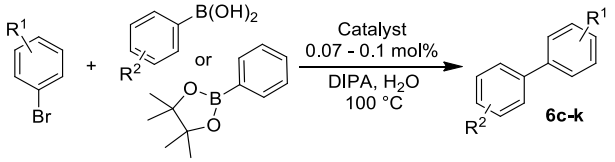

Entry	R^1	R^2	Product	t (h)	MWCNT-imi-Pd **3** Conv. (%)[b]	CNH-imi-Pd **5** Conv. (%)[b]
1	4-Ac	H	**6c**	3	99	99
2	3-Ac	H	**6d**	3	99	99
3	4-CN	H	**6e**	5	99	99
4	4-NO_2	H	**6f**	4	95	99
5	3-Me	H	**6g**	3	78	93
6	4-OMe	2-Me	**6h**	5	69	84
7	4-CHO	4-OMe	**6i**	3	99	99
8	4-Ac	-[c]	**6c**	6	81	80
9	4-OMe	4-CHO	**6j**	5	47	36
10	4-CHO	4-CHO	**6k**	24	99	99
11[d]	4-Ac	H	**6c**	16	95	99
12[e]	4-NO_2	H	**6f**	24		39

[a] Reaction conditions: aryl bromide (0.5 mmol), phenylboronic acid (0.55 mmol), DIPA (1 mmol), catalyst (0.07-0.1 mol%), H_2O (1.2 mL). [b] Conversion determined by ^1H NMR. [c] Phenylboronic acid pinacol ester was used. [d] Reaction conditions: 4-bromoacetophenone (3 mmol), phenylboronic acid (3.3 mmol), DIPA (6 mmol), catalyst (MWCNT-imi-Pd **3** 0.01 mol% or CNH-imi-Pd **5** 0.007 mol%), H_2O (3.6 mL). [e] 1-chloro-4-nitro-benzene was used.

Table 4. Comparison of catalytic activity between CNH-imi-Pd **5** and other reported catalytic systems in the Suzuki–Miyaura reaction between 4-bromoanisole and phenylboronic acid.

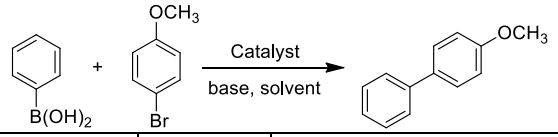

Entry	Catalyst	Pd loading (mol%)	Conditions	Time	Yield	Ref.
1	SWCNT-DETA/Pd(II)	1	K_2CO_3, H_2O/EtOH (1:1), 60 °C	1.3 h	96%	[23]
2	SWCNT-Metformine/Pd(II)	1	K_2CO_3, H_2O/EtOH (1:1), 50 °C	1 h	90%	[11a]
3	MWCNT-Schiff base/Pd(II)	0.1	K_2CO_3, H_2O/DMF (1:1), 60 °C	3 h	99%	[13a]
4	MWCNT-(*S*)-methyl histidinate/Pd(II)	0.09	K_2CO_3, H_2O/EtOH (1:1), r.t.	1 h	80%	[24]
5	SWCNT@Fe_3O_4@SiO_2/Pd	1.5	Cs_2CO_3, EtOH, 80 °C	15 h	91%	[25]
6	MWCNT/Pd	0.1	K_2CO_3, TBAB, H_2O, 120 °C	1 h	96%	[26]
7	MWCNT/Pd	0.3	Na_2CO_3, EtOH, 90 °C	8 h	99%	[27]
8	MWCNT/Pd/PdO	0.1	DIPA, H_2O, 90 °C	4 h	99%	[28]
9	Graphene/MWCNTs/Pd	0.5	K_2CO_3, H_2O/EtOH (1:1), 60 °C	1.5 h	92%	[29]
10	MWCNT-Schiff base/Pd	0.2	K_2CO_3, H_2O/EtOH (1:1), r.t.	2.5 h	92%	[30]
11	ox-SWCNH/Pd	0.05	Na_2CO_3, NMP/H_2O (2:1), 120 °C	2 h	91%	[15a]
12	Pd/C	1.5	DIPA, H_2O, 100 °C	20 min	93%	[31]
13	CNH-imi-Pd	0.07	DIPA, H_2O, 100 °C	1 h	93%	This work

Table 5. Mizoroki–Heck reactions catalyzed by materials MWCNT-imi-Pd **3** and CNH-imi-Pd **5**.[a]

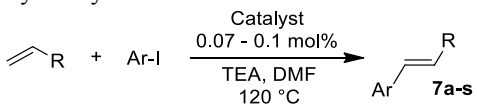

Entry	Ar	R	Product	Time (h)	Conv. (%) / [Selectivity][b]		Entry	Ar	R	Product	Time (h)	Conv. (%)[b]	
					3	**5**						**3**	**5**
1	Ph	Ph	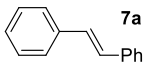 **7a**	5	99 [91]	99 [93]	11	Ph	CO_2CH_3	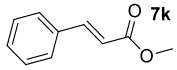 **7k**	3	99	99
2	4-MePh	Ph	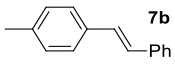 **7b**	5	86 [86]	79 [85]	12	4-MePh	CO_2CH_3	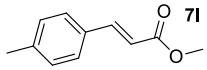 **7l**	3	99	99
3	4-OMePh	Ph	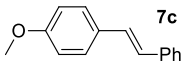 **7c**	5	87 [85]	87 [85]	13	4-OMePh	CO_2CH_3	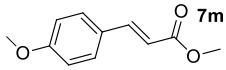 **7m**	3	99	99
4	3-OMePh	Ph	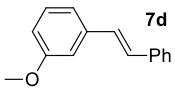 **7d**	5	90 [87]	92 [86]	14	3-OMePh	CO_2CH_3	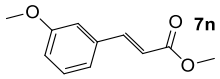 **7n**	3	99	99
5	4-AcPh	Ph	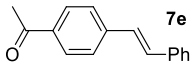 **7e**	5	91 [92]	99 [93]	15	4-AcPh	CO_2CH_3	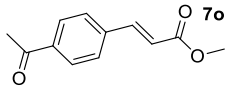 **7o**	3	99	99
6	4-NO_2Ph	Ph	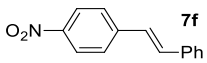 **7f**	24	63 [93]	70 [93]	16	4-NO_2Ph	CO_2CH_3	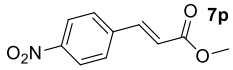 **7p**	3	99	99
7	3-BrPh	Ph	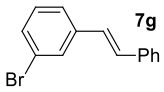 **7g**	5	86 [92]	82 [91]	17	3-BrPh	CO_2CH_3	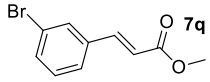 **7q**	3	94	94
8	2-Thienyl	Ph	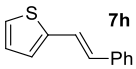 **7h**	5	81 [91]	89 [89]	18	2-Thienyl	CO_2CH_3	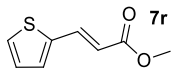 **7r**	3	99	99
9	4-AcPh	4-ClPh	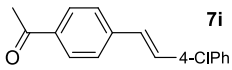 **7i**	5	99 [98]	99 [96]	19[c]	4-CHOPh	CO_2CH_3	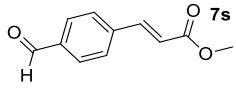 **7s**	3	99	99
10[c]	4-CHOPh	Ph	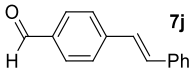 **7j**	17	81 [96]	93 [96]	20[d]	4-OMePh	CO_2CH_3	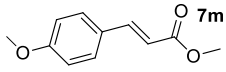 **7m**	5	99	99

[a] Reaction conditions: aryl iodide (0.5 mmol), alkene (0.75 mmol), TEA (1 mmol), catalyst (0.07-0.1 mol%), DMF (1 mL). [b] Conversion and selectivity toward *trans* alkene determined by ^{1}H NMR. [c] 4-Bromobenzaldehyde was used. [d] Reaction conditions: 4-iodoanisole (3 mmol), methyl acrylate (4.5 mmol), TEA (6 mmol), catalyst (MWCNT-imi-Pd **3** 0.01 mol% or CNH-imi-Pd **5** 0.007 mol%), DMF (3 mL).